Probing cytotoxicity of nanoparticles and organic compounds using scanning proton microscopy, scanning electron microscopy and fluorescence microscopy

Tong, Yongpeng; Li, Changming; Liang, Feng; Chen, Jianmin; Zhang, Hong; Liu, Guoqing; Sun, Huibin; Luong, John H. T.

Publisher's version / Version de l'éditeur:
https://doi.org/10.1016/j.nimb.2008.09.006
Nuclear Instruments and Methods in Physics Research B, 266, 23, pp. 5041-5046, 2008-09-12

Nuclear Instruments and Methods in Physics Research B 266 (2008) 5041–5046

Contents lists available at ScienceDirect

Nuclear Instruments and Methods in Physics Research B

journal homepage: www.elsevier.com/locate/nimb

Probing cytotoxicity of nanoparticles and organic compounds using scanning proton microscopy, scanning electron microscopy and fluorescence microscopy

Yongpeng Tong [a,*], Changming Li [b], Feng Liang [c], Jianmin Chen [d], Hong Zhang [a], Guoqing Liu [a], Huibin Sun [a], John H.T. Luong [e]

[a] Institute of Nuclear Techniques, Shenzhen University, Nanhai Avenue 3688, Shenzhen 518060, China
[b] School of Chemical and Biomedical Engineering, Nanyang Technological University, Singapore 637457, Singapore
[c] Institute Pasteur of Shanghai, Chinese Academy of Sciences, Shanghai 200025, China
[d] Shenzhen Municipal Hospital for Chronic Disease Control and Prevention, Guangdong 518020, China
[e] Biotechnology Research Institute, National Research Council Canada, Montreal, Quebec, Canada H4P 2R2

ARTICLE INFO

Article history:
Received 1 May 2008
Received in revised form 1 September 2008
Available online 12 September 2008

Keywords:
Calcium ion
Ethidium bromide
Benzo[a]pyrene
Nanoparticles
Cytotoxicity
Scanning proton microscopy

ABSTRACT

Scanning proton microscopy, scanning electron microscopy (SEM) and fluorescence microscopy have been used to probe the cytotoxicity effect of benzo[a]pyrene (BaP), ethidium bromide (EB) and nanoparticles (ZnO, Al_2O_3 and TiO_2) on a T lymphoblastic leukemia Jurkat cell line. The increased calcium ion (from $CaCl_2$) in the culture medium stimulated the accumulation of BaP and EB inside the cell, leading to cell death. ZnO, Al_2O_3 and TiO_2 nanoparticles, however, showed a protective effect against these two organic compounds. Such inorganic nanoparticles complexed with BaP or EB which became less toxic to the cell. Fe_2O_3 nanoparticles as an insoluble particle model scavenged by macrophage were investigated in rats. They were scavenged out of the lung tissue about 48 h after infection. This result suggest that some insoluble inorganic nanoparticles of PM (particulate matters) showed protective effects on organic toxins induced acute toxic effects as they can be scavenged by macrophage cells. Whereas, some inorganic ions such as calcium ion in PM may help environmental organic toxins to penetrate cell membrane and induce higher toxic effect.

1. Introduction

The toxicological effect of inorganic nanoparticles such as TiO_2 and ZnO has received significant attention [1] as they exist in aerosols [2–5]. Particulated pollutants are estimated to cause more than 500,000 annual deaths. Ultrafine air particles can easily gain access to the lung and systemic circulation where their toxic components inflict tissue damage and inflammation [1]. At the cellular level, the nanoparticles of particulate matters (PM) can penetrate into the cell and induce toxic effects. The daily mortality rate is related to the PM increase [6–8]. Aerosols induce reactive oxygen species (ROS) and inflammatory mediators, resulting in vascular permeability changes, airway constriction and tissue injury [9,10]. The transition metal ions and peroxide in aerosols can induce free radicals, resulting in both cytotoxicity and a strong oxidation response [11]. To date, most studies focus on the effect of nanoparticles per se [4] without considering their interaction with organic pollutants although they often coexist as aerosol which can be inhaled by human beings. Nanoparticles, found in macrophages, can induce mitochondrial damage [5]. The acute effects of aerosols might be mainly due to soluble metal ions [12]. However, the main contributing components of ultrafine particles (UFP) such as organic and/or inorganic toxins have not been investigated.

As ultrafine air particles can easily gain access to the lung and systemic circulation and induce cytotoxicity of T cell, the cytotoxicity experiments can use T lymphoblastic leukemia Jurkat cell line as a good model. This study focuses on the cytotoxicity of three common nanoparticles: ZnO, Al_2O_3 and TiO_2, in the presence or absence of two carcinogenic agents, benzo[a]pyrene and ethidium bromide (BaP and EB) on a T lymphoblastic leukemia Jurkat cell line cultured under various calcium ion concentrations. BaP and EB were selected as the test models since a vast number of studies over the previous three decades have documented a link between BaP and cancers [13]. EB, commonly used to detect nucleic acids [14], is suspected to be carcinogenic and teratogenic because of its mutagenicity.

2. Materials and methods

2.1. Cell toxicity in the presence of inorganic particles and calcium ion

2.1.1. Stimulation by calcium ion

RPMI-1640 (containing 0.42 mM Ca^{2+}), ethidium bromide (EB) and benzo[a]pyrene (BaP) were purchased from MP Biomedicals

* Corresponding author. Fax: +86 755 26534374.
E-mail address: yongpengt@yahoo.com.cn (Y. Tong).

0168-583X/$ - see front matter © 2008 Elsevier B.V. All rights reserved.
doi:10.1016/j.nimb.2008.09.006

(Irvine, CA). Nanopowders (ZnO and TiO_2, 99.9% purity) were from Aldrich whereas Al_2O_3 was purchased from CH Instruments (Austin, TX). Those inorganic particles can be formed stable water suspension at pH 7 and their average size distribution is 50–200 nm in diameter. Human Jurkat (clone E6-1) T lymphocyte line was obtained from the Institute of Biochemistry and Cell Biology, Shanghai, China. The cells were grown on a RPMI-1640/10% FCS medium in a 48-well plate, each well contained 290 μl medium with $\sim 5 \times 10^4$ cells. Different concentrations of EB, BaP, ZnO and TiO_2 and Al_2O_3 suspension and Ca^{2+} (the Ca^{2+} concentration was regulated by adding $CaCl_2$ solution at pH 7) were added and PBS was used as control. After 20 h incubation at 37 °C under 5% CO_2, the cells were collected by centrifugation and resuspended in 300 μl PBS. The cell suspension of each sample was used for the MTT (3-(4, 5-dimethylthiazolyl-2)-2, 5-diphenyltetrazolium bromide) assay to estimate the cell survival rate. The whole process of the EB accumulation inside the cell was monitored by fluorescence microscopy (Leica FC300FX, excitation: 300–365 nm, emission <510 nm, acquired time: 540 ms, 9.8×, color saturation 1.35×). A typical ZnO particles on Si surface and ZnO particles suspension has been analyzed by SEM and Nicomp 380/ZLS (Zeta Potential Analyzer) respectively.

3. Scavenge of inorganic particles

3.1. Ferric oxide intratracheal instillation experiment

Spraque-Dawley (SD) rats, free of known rodent pathogens, (from the National Rodent Laboratory Animal Resources, Shanghai Branch) weighing 200 ± 10 g were used. They were selected because of their calmness and ease of handling. They received a standard pellet diet and water. Experimental rats were randomly divided into six groups with four male rats per group. Four groups were instilled from trachea with 0.2 ml ferric oxide particle suspension (10 mg/kg body weight) to obtain tissue sections at different times. One group was instilled with PBS (Phosphate Buffered Saline), as control and the four remaining groups received no treatment (placebo). Tissue sections were divided and analyzed by SPM and SEM, respectively. The procedures were performed in accordance with the recommendations in the Guide for the Care and Use of Laboratory Animals published by the National Institutes of Health (NIH, Bethesda, MD).

3.2. SPM analysis

Micro-PIXE measurement was performed using a 2.25 MeV proton beam focused to 1 μm. For the ion beam measurement, the current was about 6–9 pA and the typical collected charge was about 0.60 μC. The typical resolution of images of elemental distributions from PIXE analysis was 1 μm. The elemental distribution was obtained by the Geo-PIXE procedure.

4. Results and discussion

4.1. Cytotoxicity of EB and BaP

EB 30 μl (5 mg/ml) was added to the culture medium (1 ml) containing $\sim 2 \times 10^5$ Jurkat cells and after 60 min and 80 min of incubation, the effectors were examined by fluorescent microscopy. As shown in Fig. 1, EB was able to penetrate the cell membrane, followed by its inward movement and accumulation in the nucleus. BaP also exhibited acute toxicity on the cell as anticipated from the well-known toxicity of this five ring polyaromatic hydrocarbon. BaP was first determined in 1933 as a component of coal tar that was responsible for the first recognized occupation-associated cancers. It induces vitamin A deficiency in rats and is mutagenic and highly carcinogenic. Notice also that cytotoxicity induced by EB and BaP became more pronounced if the cultured medium contained an elevated level of Ca^{2+} (0.42–20 mM) as shown in Table 1. Such a finding was somewhat surprising since Ca^{2+} up to 20 mM exhibited no toxic effects on Jurkat T lymphocyte cells (designated as 11 in Table 1).

The apoptosis event was monitored by taking photos of the cells which were exposed to a relatively high concentration of EB (200 μg/ml) with different concentrations of Ca^{2+} (Fig. 2). After 10 min exposure, no significant EB accumulation was noticed and these cells were transparent in optical microscopy with their viability confirmed by the Trypan blue exclusion test. After 60–90 min, the intracellular fluorescent intensity increased signifi-

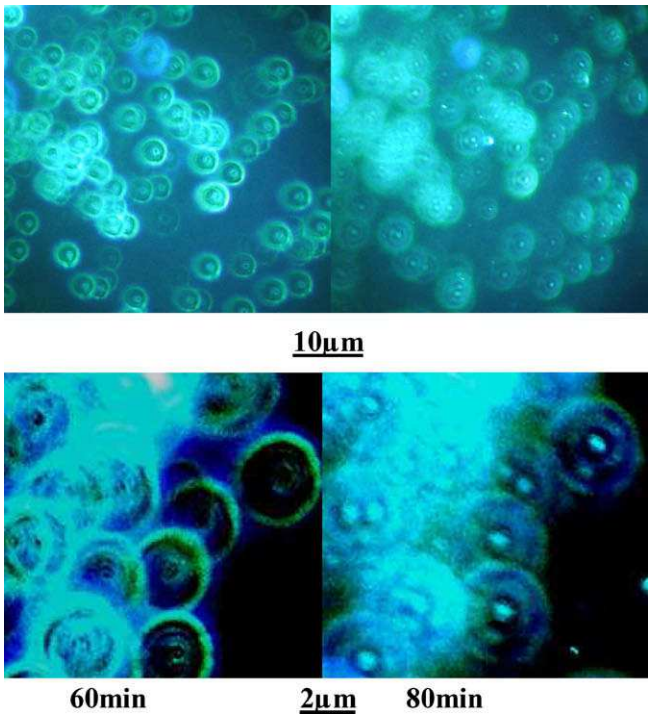

Fig. 1. Jurkat cell incubated with EB at 60 min and 80 min later.

Table 1
The Jurkat cell survivor rate after 20 h incubation with different formation of environmental toxin BaP and EB

Cultured condition	Survivor rate	*p* value
(1) Control (300 μl cells) (0.42 mM Ca^{2+})	100%	
(2) 60 μg/ml BaP (0.42 mM Ca^{2+})	87% + 6%	<0.05 (compared with the control)
(3) 60 μg/ml BaP (5 mM Ca^{2+})	85% + 5%	<0.05 (compared with the control)
(4) 60 μg/ml BaP (10 mM Ca^{2+})	75% + 3%	<0.05 (compared with (2))
(5) 60 μg/ml BaP (20 mM Ca^{2+})	60% + 5%	<0.05 (compared with (2))
(6) 60 μg/ml EB (0.42 mM Ca^{2+})	75% + 3%	<0.05 (compared with the control)
(7) 120 μg/ml EB (0.42 mM Ca^{2+})	70% + 4%	<0.05 (compared with the control)
(8) 60 μg/ml EB (5 mM Ca^{2+})	69% + 5%	<0.05 (compared with (6))
(9) 60 μg/ml EB (10 mM Ca^{2+})	60% + 4%	<0.05 (compared with (6))
(10) 60 μg/ml EB (20 mM Ca^{2+})	50% + 6%	<0.05 (compared with (6))
(11) (20 mM Ca^{2+})	95% + 7%	>0.5% (compared with the control)

The sample number is 6 and the *p* value is calculated from student's *t*-test.

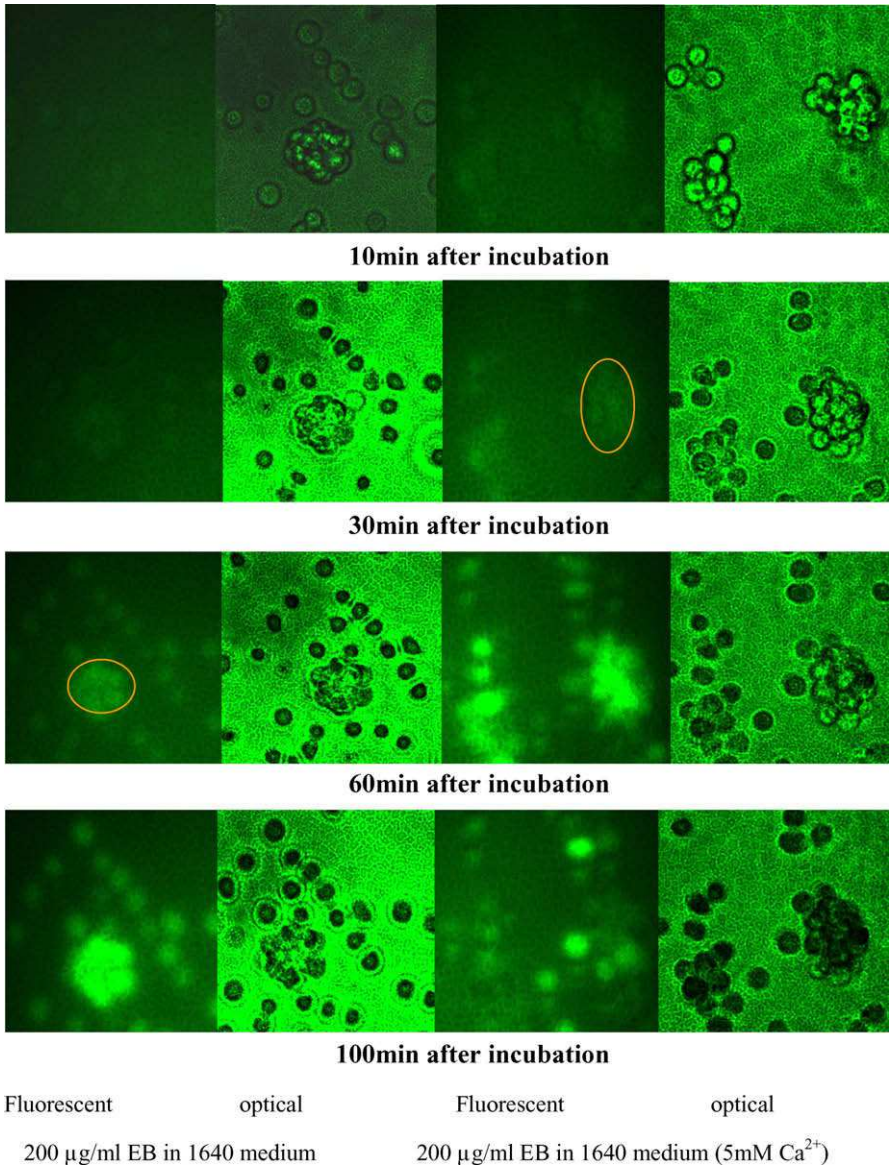

Fig. 2. The typical photos of Jurkat T lymphocyte cells under toxin EB (200 μg/ml) with 0.42 mM and 5 mM Ca^{2+} in 1 ml culture medium at different cultured time.

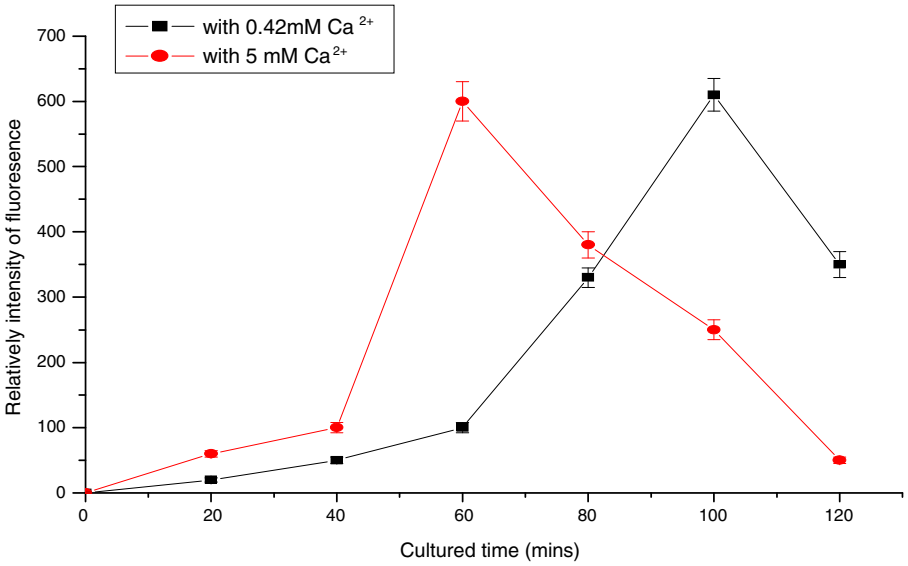

Fig. 3. The relatively intensity of fluorescence of marked cell clusters at different cultured time under toxin EB (200 μg/ml) with 0.42 mM and with 5 mM Ca^{2+}, respectively.

Table 2
The Jurkat cell survivor rate after 20 h incubation with different formation of environmental toxin BaP

Cultured condition	Survivor rate	*p* value
(1) Control (300 μl cultured cells)	100%	
(2) 100 μg/ml ZnO	93% + 6%	>0.5 (compared with the control)
(3) 100 μg/ml Al_2O_3	94% + 5%	>0.5 (compared with the control)
(4) 100 μg/ml TiO_2	96% + 3%	>0.5 (compared with the control)
(5) 60 μg/ml BaP	60% + 5%	<0.05 (compared with the control)
(6) 120 μg/ml BaP	40% + 7%	<0.05 (compared with the control)
(7) 60 μg/ml BaP, 100 μg/ml ZnO	85% + 6%	<0.05 (compared with (5))
(8) 60 μg/ml BaP, 100 μg/ml Al_2O_3	83% + 4%	<0.05 (compared with (5))
(9) 60 μg/ml BaP, 100 μg/ml TiO_2	71% + 6%	<0.05 (compared with (5))

The number of samples is 6 and the *p* value is calculated from student's *t*-test.

cantly and such a result was not totally unexpected since this intercalating agent is commonly used as a nucleic acid stain (Fig. 3). When exposed to ultraviolet light, it will fluoresce with a red-orange color, intensifying almost 20-fold after binding to DNA. Further prolonged incubation resulted in a rapid decrease in the fluorescence intensity and stained cells became black as evidenced by optical microscopy, an indicator of cell death. After 120 min, a majority of cells turned to black as revealed by optical microscopy and failed to transform MTT. In brief, MTT is reduced by active cells, in part by the action of dehydrogenase enzymes, to generate reducing equivalents such as NADH and NADPH. Experimental data also confirmed that the penetration of EB, leading to cell death, was more rapid at high Ca^{2+} concentrations.

4.2. Cytotoxicity of EB and BaP in the presence of nanoparticles

ZnO, TiO_2 and Al_2O_3 nanoparticles below 0.1 mg/ml exhibited no appreciable cytotoxicity on the cell (Table 2). TiO_2 was considered here since it is the most commonly manufactured and most promising nanoparticle, being used for a variety of applications from self-cleaning surfaces to water purification. Only minimal toxicological effects have been reported for macrophages exposed as high as 500 μg/ml Al_2O_3-nanoparticles for 24 h. However, a significant delayed toxicity occurred at 96 and 144 h post exposure. Therefore, a series of experiments was conducted to evaluate the cytotoxicity of 10 μl BaP in the presence of such nanoparticles at this level. The survival rate increased more than 10% (from 60% in formation (5) to 71, 83 and 85%, respectively in formation (7), (8), (9), cultured in the presence of ZnO, TiO_2, Al_2O_3 nanoparticles, respectively). This was an important finding since inorganic nanoparticles often coexist and interact strongly with organic pollutants. Although there are several reports on nanoparticle induced cell toxic effects [3–8], there is little information about the combined effects of inorganic nanoparticles coexisting with environmental pollutants. It was reasoned that BaP was absorbed by nanoparticles mainly via hydrophobic interaction to form a BaP-nanoparticle complex which became less toxic to the cell. As particles in the cardiopulmonary system are most often ingested by phagocytes, the organic pollutant-nanoparticle complex can be more easily scavenged compared to individual organic compounds.

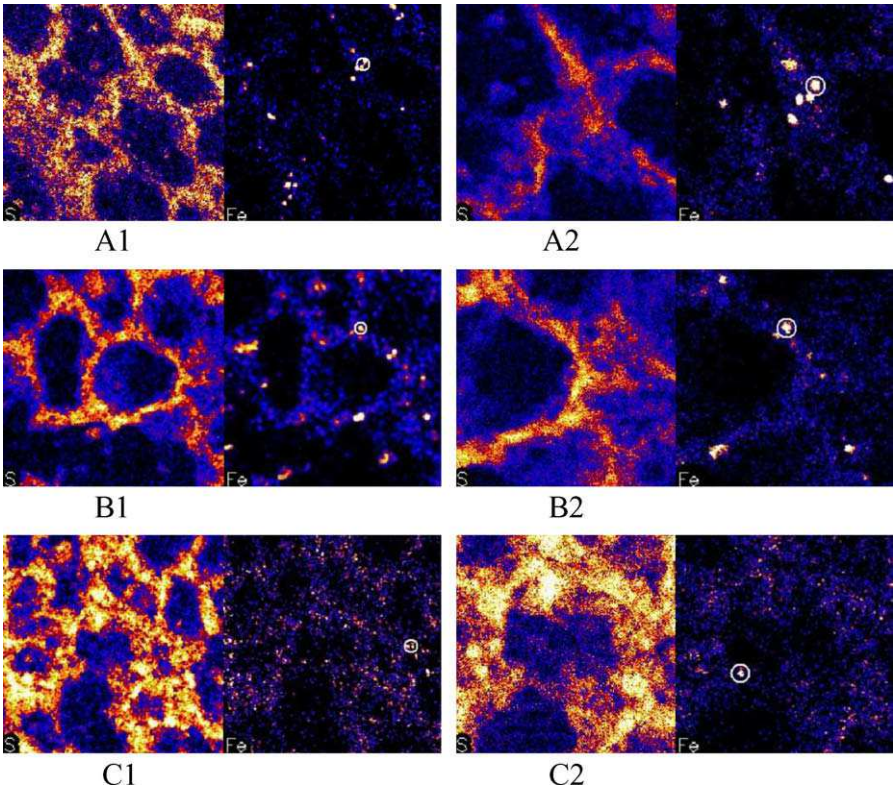

Fig. 4. Typical S and Fe distributions of lung tissue sections after intratracheal instillation at different time: A1: 6 h, (scan area *X* = 0.100 mm, *Y* = 0.100 mm) A2: 6 h, (scan area *X* = 0.050 mm, *Y* = 0.050 mm) B1: 24 h, (Scan area *X* = 0.100 mm, *Y* = 0.100 mm) B2: 24 h, (scan area *X* = 0.050 mm, *Y* = 0.050 mm) C1: 48 h, (scan area *X* = 0.100 mm, *Y* = 0.100 mm) C2: 48 h, (scan area *X* = 0.0500 mm, *Y* = 0.0500 mm), (circle marked areas are ferric oxide particles).

Table 3
Elemental contents of lung tissue by SPM

Sampleno. (h)	Alveolar septal position			Particle position in 3 μm circle		
	P μg/g	S μg/g	Fe μg/g	P μg/g	S μg/g	Fe μg/g
6	1190 + 100	2240 + 150	150 + 30	1400 + 250	2300 + 300	4500 + 1000
24	1850 + 400	3530 + 500	290 + 90	2000 + 500	3500 + 500	3900 + 900
48	1650 + 250	2510 + 400	220 + 50	3300 + 700	3600 + 500	700 + 200[a]

[a] The number of detected samples of each group is 5 and there is a significant difference ($p < 0.05$) (compared with the concentration in group 6 h, or group 24 h).

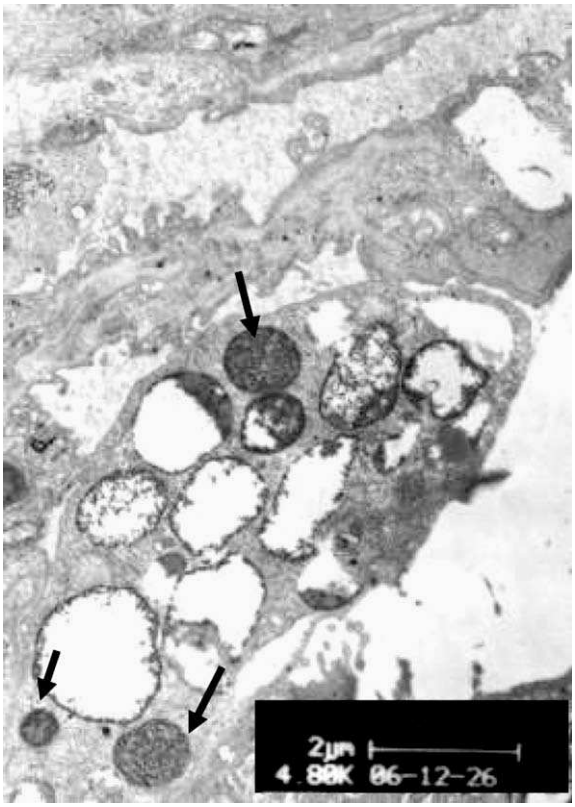

Fig. 5. A typical SEM scanning of lung tissue section of 24 h after installation of ferric oxide particles (arrow marked areas are ferric oxide particles).

It is well known that the changes in the cytoplasmic calcium concentration ($[Ca^{2+}]i$) regulate a wide variety of cellular processes. External calcium can change intracellular calcium in normal and neoplastic keratinocytes [15]. Ca^{2+} has a role in cell injury that appears to uniquely involve mitochondrial homeostasis [16]. The extracellular calcium level is normally about 1–3 mM compared to 0.1–0.27 μM of its intracellular counterpart. A variety of membrane transport-channels regulate calcium homeostasis and modulate cell responses to environmental stimuli. Damage to calcium transport channels or the integrity of the cell membrane results in the rapid influx of calcium. A major contributor to cell membrane damage is lipid peroxidation that is initiated by oxidative stress. When membrane damage elevates the intracellular concentration of calcium above 0.5 μM, mitochondria begins to work to remove calcium from the cytoplasm. The sufficiently high level of calcium inside cells will mediate a cascade of destructive events including the disruption of enzyme functions, ion and pH balances and alterations in the functions of critical organelles including the mitochondria, leading to apoptosis. If organic toxins induced higher TNF (tumor necrosis factor), higher external Ca induces higher intracellular Ca^{2+} ions, resulting in cell death. It is reported that the cultured macrophage cells exposed continuously to a well-defined model of PM benzo[a]pyrene adsorbed on carbon black (CB and BaP)] exhibit a time-dependent expression and release of the cytokine TNF. TNF mediates PM-induced apoptosis and the MAPK (Mos/mitogen-activated protein kinase) pathway might play an important role in this pathway [17]. Thus, the external Ca accelerates cell death owing to TNF mediated cell death when organic toxins exist. The external Ca may have another way to accelerate cell death by stimulating cells to accumulate environmental toxins. Usually, the exchange of substances across cellular membranes may be accomplished by diffusion, facilitated diffusion, or active transport. The result of unaided diffusion is an equilibration of concentrations on both sides of the membrane. In facilitated diffusion,

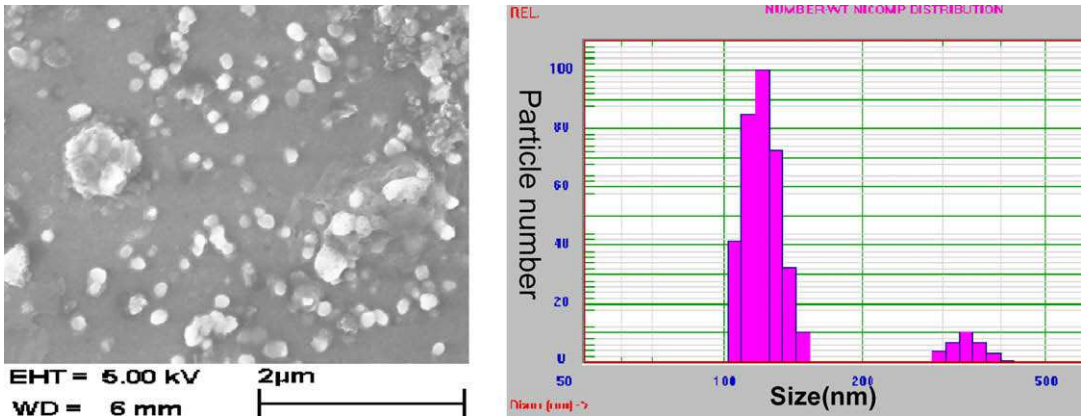

Fig. 6. A typical SEM scanning (left) and a typical analysis by Nicomp 380/ZLS (Zeta Potential Analyzer) (right) of ZnO particles on Si surface and on ZnO particles suspension, respectively.

the establishment of equilibrium is accelerated by the function of a protein. Active transport is necessary to accumulate a substance against a concentration gradient. Thermodynamics requires energy to perform this task, so there has to be another downhill gradient that may be dissipated or some other form of chemical energy such as transport ATPases and sodium pumps utilizing decarboxylation energy. Nutrients as well as toxins can be transported into the cell by the downhill or uphill gradient state. From our result, environmental toxins were accumulated in cell against a concentration gradient and external calcium stimulated the process. Due to the accumulation of organic toxins, cells failed the Trypan Blue exclusion test, confirming their non-viability.

4.3. Animal experiments of scavenge of inorganic particles

Fe ions induce toxicity in lung tissues [18] and Fe_2O_3 particles can be identified by optical microscopy, SPM and SEM. The histopathological changes in the lungs of different rat groups have been reported in the literature [18]. Black ferric oxide particles were found in alveolar but we could not ascertain the difference between ferric oxide particles with other deposits including carbon and the scavenging process of such particles with time. Fe_2O_3 particles were used in this study as a model of scavenge. When those particles were scavenged, the absorbed organic toxin on particles and the source of toxic ions were scavenged as well.

4.3.1. SPM scanning

Fig. 4 illustrates that S and Fe element distributions changed with different time after instillation. Six hours into the experiment, ferric oxide particle (white spots in Fe image in circle area) deposition was present in alveolar walls (A1, A2) and within 24 h (B1 and B2), the ferric oxide particles were not significantly scavenged. However, after 48 h the level of the ferric oxide particles decreased drastically as no white spot was observed in the Fe image (C1 and C2). The alveolar wall was thickened; an obvious characteristic of lung inflammation and usually at this time, a lot of alveolar macrophages would be present. Thus, the ferric oxide particles would be scavenged by macrophages. Inflammation might be induced by the ferric oxide particles and help to scavenge the ferric oxide particles from lung tissue. As shown in Table 3, the Fe concentration after 48 h in the 3 μm circle area (Fig. 4) decreased significantly. At this time, Fe_2O_3 particles should be phagocytized by pulmonary macrophages and eliminated from lung tissue [15,16].

4.3.2. SEM scanning

Twenty-four hours after instillation, most ferric oxide particles were within macrophage cells as shown in Fig. 5, implying that the scavenge of Fe_2O_3 particles was phagocytized by macrophage cells. Furthermore, ferric oxide particles (2.6 μm) were phagocytized by pulmonary macrophages and induced lung inflammation, 24 h after intrapulmonary instilled ferric oxide particles [19]. As reported, the particles instilled in pulmonary cell can be phagocytized within 6–12 h and scavenged [3]. The dynamics of scavenging particles (5 μm) from human pulmonary has also been reported [20]. Some biological targets of inhaled PM are the pulmonary epithelium and resident macrophages. Blood cells are also the target as nanoparticles and organic toxins penetrate into blood. Insoluble particles (Fe_2O_3, $CaCO_3$, CaO, etc.) can produce ions and induce higher toxicity in lung tissue [10] under high acid environment.

A typical SEM scanning and a typical detection by Nicomp 380/ZLS (Zeta Potential Analyzer) of ZnO particles on Si surface and on ZnO particles suspension respectively have been analyzed and showed on Fig. 6. Most ZnO particles are 100–160 nm in diameter.

Our results demonstrated that inorganic nanoparticles with organic environmental toxins exhibited less toxic effects than such toxins alone per se on T lymphocyte cells. The integrative progress of inorganic particles may act as a protective progress when organic toxins exist. In contrast, elevated calcium facilitated the penetration of organic toxins to the cell membrane and induced higher toxic effects.

5. Funding

National Science Foundation of China (10675159) (10775099), Nanyang Technological University and Guangdong Provincial Natural Science Fondation of China (7301362).

Acknowledgments

The PIXE measurement was done at Fakultät für Physik und 10 geowissenschaften, Universität Leipzig with the help of Professor Tilman Butz and Dr. Tilo Reinert. The authors declare that they have no competing financial interests.

References

[1] A. Nel, T. Xia, T. Madler, N. Li, Toxic potential of materials at the nanolevel, Science 311 (2006) 622.
[2] J. Kaiser, Evidence mounts that tiny particles can kill, Science 289 (2000) 22.
[3] G. Oberdörster, E. Oberdörster, J. Oberdörster, Nanotoxicology: an emerging discipline evolving from studies of ultrafine particles, Environ. Health Perspect. 11 (2005) 3823.
[4] A. Khandoga, A. Stampfl, S. Takenaka, H. Schulz, R. Radykewicz, W. Kreyling, F. Krombach, Ultrafine particles exert prothrombotic but not inflammatory effects on the hepatic microcirculation in healthy mice in vivo, Circulation 109 (2004) 1320.
[5] A. Nel, Air pollution-related illness: effects of particles, Science 308 (2005) 804.
[6] A. Bhatnagar, Environmental cardiology: studying mechanistic links between pollution and heart disease, Circ. Res. 99 (2006) 692.
[7] N. Pierse, L. Rushton, R.S. Harris, C.E. Kuehni, M. Silverman, J. Grigg, Locally generated particulate pollution and respiratory symptoms in young children, Thorax 61 (2006) 216.
[8] J. Wan, D. Diaz-Sanchez, Phase II enzymes induction blocks the enhanced IgE production in b cells by diesel exhaust particles, J. Immunol. 177 (2006) 3477.
[9] U.P. Kodavanti, R.H. Jaskot, W.Y. Su, D.L. Costa, A.J. Ghio, K.L. Dreher, Genetic variability in combustion particle-induced chronic lung injury, Am. J. Physiol. 272 (1997) L521.
[10] Y. Tong, X. Ni, Y. Zhang, F. Chen, G. Zhang, S. Ye, The study of toxicological mechanism of acidified aerosols, Biol. Trace Elem. Res. 85 (2002) 149.
[11] K. Donaldson, D.M. Brown, C. Mitchell, M. Dineva, P.H. Beswick, P. Gilmour, W. MacNee, Free radical activity of PM10: iron-mediated generation of hydroxyl radicals, Environ. Health Perspect. 105 (Suppl. 5) (1997) 1285.
[12] I.Y.R. Adamson, H. Prieditis, R. Vincent, Pulmonary toxicity of an atmospheric particulate sample is due to the soluble fraction, Toxicol. Appl. Pharmacol. 157 (1999) 43.
[13] M.F. Denissenko, A. Pao, M. Tang, G.P. Pfeifer, Preferential formation of benzo[a]pyrene adducts at lung cancer mutational hotspots in P53, Science 18 (1996) 430.
[14] Q. Huang, W.L. Fu, Comparative analysis of the DNA staining efficiencies of different fluorescent dyes in preparative agarose gel electrophoresis, Clin. Chem. Lab. Med. 43 (8) (2005) 841.
[15] H. Hennings, F.H. Kruszewski, S.H. Yuspa, R.W. Tucker, Intracellular calcium alterations in response to increased external calcium in normal and neoplastic keratinocytes, Carcinogenesis 10 (1989) 777.
[16] D.J. Reed, G.A. Pascoe, C.E. Thomas, Extracellular calcium effects on cell viability and thiol homeostasis, Environ. Health Perspect. 84 (1990) 113.
[17] B.Y. Chin, M.E. Choi, M.D. Burdick, R.M. Strieter, T.H. Risby, A.M.K. Choi, Induction of apoptosis by particulate matter: role of TNF- and MAPK, Am. J. Physiol. Lung Cell Mol. Physiol. 275 (1998) L942.
[18] Y. Tong, G. Zhang, Y. Li, M. Tan, W. Wang, J. Chen, P. Hwu Hsu, J.H. Je, G. Margaritondo, W. Song, R. Jiang, Z. Jiang, Synchrotron microradiography study on acute lung injury of mouse caused by PM2.5 aerosols, Eur. J. Radiol. 58 (2) (2006) 266.
[19] J.C. Lay, W.B. Bennett, C.S. Kim, R.B. Devlin, P.A. Bromberg, Retention and intracellular distribution of instilled iron oxide particles in human alveolar macrophages, Am. J. Respir. Cell Mol. Biol. 18 (1998) 687.
[20] D.V. Booker, A.C. Chamberlain, D.J. Rundo, C.F. Muir, Elimination of 5 μm particles from the human lung, Nature 215 (1967) 30.